doi.org/10.36721/PJPS.2020.33.6.REG.2667-2677.1

Green synthesis of hesperidin coated silver nanoparticles for colorimetric detection of gentamicin sulfate in real samples

Saira Yasmeen[1], Muhammad Imran[2], Muhammad Raza Shah[2] and Munawwer Rasheed[3]*

[1]Department of Chemistry, University of Karachi, Karachi, Pakistan
[2]H.E.J. Research Institute of Chemistry, International Center for Chemical and Biological Sciences, University of Karachi, Pakistan
[3]Centre of Excellence in Marine Biology, University of Karachi, Karachi, Pakistan

Abstract: Gentamicin sulfate (GEN), a well-known broad-spectrum antibiotic is mostly administered through intramuscular injections and entirely excreted in un-metabolized form through urination from patient's body. Quantitative detection of GEN by direct UV absorption is usually challenging due to lack of chromophores and fluorophores in structure. The current study described the hesperidin coated silver nanoparticles (HSPAgNPs) based novel colorimetric quantitative assay for GEN. HSPAgNPs, based colorimetric detection involved a transition from characteristic yellow colour to blackish brown upon addition of GEN, accompanied by a significant quenching in localized surface plasmon resonance (LSPR) band at λ_{max} 398 nm. Moreover, the synthesized HSPAgNPs were employed to rapid and quantitative detection of GEN in concentration range of 5 to 100 µM. Limit of detection (LOD) and limit of quantification (LOQ) was calculated by standard deviation of the ordinate intercept and slope of the regression line and estimated to be 6.89 µM and 20.88 µM respectively, with a linear correlation factor R^2 equal to 0.9990 which strictly followed Beer's law. Furthermore, the utility and effectiveness of HSPAgNPs was also explored for selective recognition of GEN in tap water, serum, human blood plasma and urine.

Keywords: Green synthesis, hesperidin coated silver nanoparticles, molecular recognition ability, colorimetric detection, gentamicin sulfate.

INTRODUCTION

In many developed as well as developing countries the amount of pharmaceutical drugs released in water is becoming alarming these days (Scheurell *et al.,*2009; Selke *et al.,* 2010). Daily a variety of antibiotic drugs are released from hospital effluents to drainage system. This plays a significant role in enhancement of bacterial resistance (Wise *et al.,* 1998). If constantly alarming concentrations remain to release the municipal sewage, sewage treatment plants may become a reservoir of resistant bacteria (Hartmann *et al.,* 1999).

Due to lack of proper sewage treatment the amount of released antibiotic substances eventually become a threat to aquatic life and its user. Antibiotics containing different functional groups such as β-lactams, quinolons or sulfonamides are not readily biodegradable (Al-Ahmad *et al.,* 1999; Ingerslev and Halling-Sørensen, 2000; Kümmerer *et al.,* 2000a). Which indicates that biodegradation does not play an important role in elimination of these active moieties. In this scenario an active and non-biotic proper degradation protocol including hydrolysis, adsorption deactivation or cleavage by enzymes is necessary for the elimination of antibiotic substances in sewage treatment plants and hospital effluents (Kümmerer *et al.,* 2000b). Therefore, it is indispensible to develop an appropriate method for monitoring of these antibiotics in water bodies.

**Corresponding author:* e-mail: rasheed.munawwer@uok.edu.pk

Aminoglycosides (AGs) are a class of broad-spectrum antibiotics (ABs), which are well known for therapeutic and veterinary applications. Because of availability and low cost, AGs are extensively used. Therefore, their residues are found abundantly in environment (Greenwood *et al.,* 2007; Zhu *et al.*, 2013). Gentamicin sulfate, (2R,3R,4R,5R)-2-[(1S,2S,3R,4S,6R)-4,6-diamino-3-[(2R,3R,6S)-3-amino-6-[(1R)-1-(methylamino)ethyl] oxan-2-yl]oxy-2-hydroxycyclohexyl] oxy-5-methyl-4-(methyl-amino)oxane-3,5-diol; sulfuric acid (GEN), an AG, is commonly used to cure and prevent variety of bacterial infections. Mostly administered through intramuscular injections and excreted out from a body in un-metabolized form (Löffler and Ternes, 2003). Additionally, potent antimicrobial efficacy of GEN causes reversible-nephrotoxicity and irreversible-ototoxicity. Moreover it is also reported for ataxia, dizziness, nystagmus and primarily vestibulotoxicity (Selimoglu, 2007).

Quantitative detection of GEN by direct UV absorption is usually challenging due to lack of chromophores and fluorophores in structure. Varieties of analytical methods are reported for determination of AGs based on separations by liquid chromatography mass spectrometry (LC–MS) including HILIC–MS/MS, high–pH RPLC–MS, capillary electrophoresis, ion–pair liquid chromatography and thin layer chromatography. More recently developed or improved techniques involved an

ion spray high-performance liquid chromatography coupled with tandem mass spectrometry (HPLC/MS/MS) have also been employed. However, these cutting edge techniques are not accessible in less developed countries due to high instrumentation cost (Farouk *et al.,* 2015; Heller *et al.,* 2000; McLaughlin and Henion, 1994).

Noble metal nanoparticles (NPs), specially silver and gold, exhibit significant optical properties. The combined oscillation of electrons from valance band to a conduction band produce a characteristic localized surface plasmon resonance (LSPR) band in visible region (380-750 nm), after interaction with EMR. This optical response of nanoparticles made these appealing candidates for chemosensing. Optical response of these nanosensors depends on dimension, morphology and local refractive index of NPs. During recognition process, the LSPR band of NPs shifts in response to their environment by interacting with analyte molecules. These interactions include hydrogen bonding, π–π stacking, host guest interaction, Vander Waals forces, electrostatic interaction, charge transfer and antigen-antibody interactions have already been studied in detail (Boal *et al.,* 2000; Caruso et *al.,* 1998; Jin *et al.,* 2001; Liu *et al.,* 1999; Naka *et al.,* 2003; Patil *et al.,*1997; Shenton *et al.,* 1999) .

Various natural products such as flavonoids, alkaloids, terpenoids, polyphenols, proteins, and polysaccharides and synthetic compounds such as macromolecules are reported for functionalization and stabilization of NPs (Fang *et al.,* 2011).The elementary step for synthesis of nanoparticles involves the reduction of metallic salts in the presence of reducing agent. Usually these reducing agents are not capable to flourish the eco-friendly behaviour and ultimately lead to specific toxicities. "Green Synthesis" refers to explore the methods for the synthesis of nanoparticles using environment friendly approaches (Anastas and Warner, 2000).

The aim of current study is to proposed an environment friendly, one-pot robust, reproducible and cost effective analytical protocol for synthesis of silver nanoparticles (AgNPs) stabilized with a flavonoid, hesperidin, (3′,5,7-trihydroxy-4′-methoxy-flavanone-7-O-β-rutinoside HSP). HSP is mainly found in many species of genus citrus e.g., *Citrus reticulata* and *Citrus sinensis* (Aghel *et al.,*2008). HSP is reported for anti-inflammatory, cholesterol reduction, vasoprotective, antioxidant, hypolipidemic and anticarcinogenic activities. HSP also induces the inhibition of HMG-CoA reductase, phospholipase A2, cyclo-oxygenase and lipoxygenase (Inoue *et al.,* 2002).

Moreover, in addition to these striving features HSP induces remarkable potential in reduction of silver ions for the fabrication of AgNPs. Hence, it can be affirmed that HSP based nanosensor (HSPAgNPs) will ultimately contribute astonishing optical characteristics which can be explored in several dimensions. Herein, we are reporting a new synthetic approach which offers an optical nanosensor (HSPAgNPs) for selective recognition and ultra-trace detection of GEN in water and biological fluid.

MATERIALS AND METHODS

Analytical grade solvents and reagents i.e., silver nitrate ($AgNO_3$), azithromycine ($C_{38}H_{72}N_2O_{12}$), carbamuzeplue ($C_{15}H_{12}N_2O$), cefixime ($C_{16}H_{15}N_5O_7S_2$), ceftriaxone sodium ($C_{18}H_{16}N_8Na_2O_7S_3$), cefuroxime ($C_{16}H_{16}N_4O_8S$), cefaclor ($C_{15}H_{14}ClN_3O_4S$), cephalexin micronized ($C_{16}H_{17}N_3O_4S.\ H_2O$), clarithromycin ($C_{38}H_{69}NO_{13}$), clindamycin phosphate ($C_{18}H_{33}ClN_2O_5S$), diclofenac sodium ($C_{14}H_{10}C_{l2}NNaO_2$), flurbiprofen ($C_{15}H_{13}FO_2$), fluconazole ($C_{13}H_{12}F_2N_6O$), GEN as gentamicin sulfate ($C_{21}H_{43}N_5O_7.H_2SO_4$), phenobarbital ($C_{12}H_{12}N_2O_3$), prednisolon ($C_{21}H_{26}O_5$) and theophylline ($C_7H_8N_4O_2$) were purchased from sigma Aldrich. As per routine, all the glassware were washed with aqua regia followed by deionized water.

Isolation and purification of HSP

Pritchett and Merchant (Pritchett and Merchant, 1946) were followed to isolate HSP. In short, 200g sun dried and disintegrated orange peel (*C. reticulata*) were refluxed with 1 L of petroleum ether on a water bath for 1 h and then contents were hot filtered through buchner funnel. The dry residue was again refluxed for 3h using 1 L of methanol and then filtered while hot followed by washing with hot methanol (200ml). Filtrate was concentrated on rotary evaporator then resultant syrupy residue was collected in (5.0ml) dilute acetic acid and allowed to stand for crystallization, yielding white needles; m.p. 252-254°C.

A 10% solution of HSP in formamide was prepared by warming and treated with previously boiled (using diluted HCl for 30 min) activated charcoal. The acidified solution was filtered via celite and allowed to stand for crystallization after dilution with H_2O. The resulting crystals were than filtered off followed by washing with hot H_2O and isopropanol affording pure white crystalline product m.p. 261-263°C.

Synthetic protocol for HSPAgNPs

The green synthesis of HSPAgNPs accomplished by drop wise addition of 0.1mM aqueous solution (10 ml) of HSP into 100 ml of 0.1mM aqueous solution of $AgNO_3$ with constant stirring at 50-60°C. Gentle heating gradually turned the colour of reaction mixture from colourless to yellow indicating significant reduction of pure Ag^{+1} ions to Ag° and formation of HSPAgNPs (Saxena *et al.,* 2012).

Determination of stability of HSPAgNPs

Sustainability of HSPAgNPs was investigated against heat, pH and electrolytic effect of NaCl. In order to find out the stability of HSPAgNPs against heat, about 2.0 ml solution of HSPAgNPs was subjected to continuous

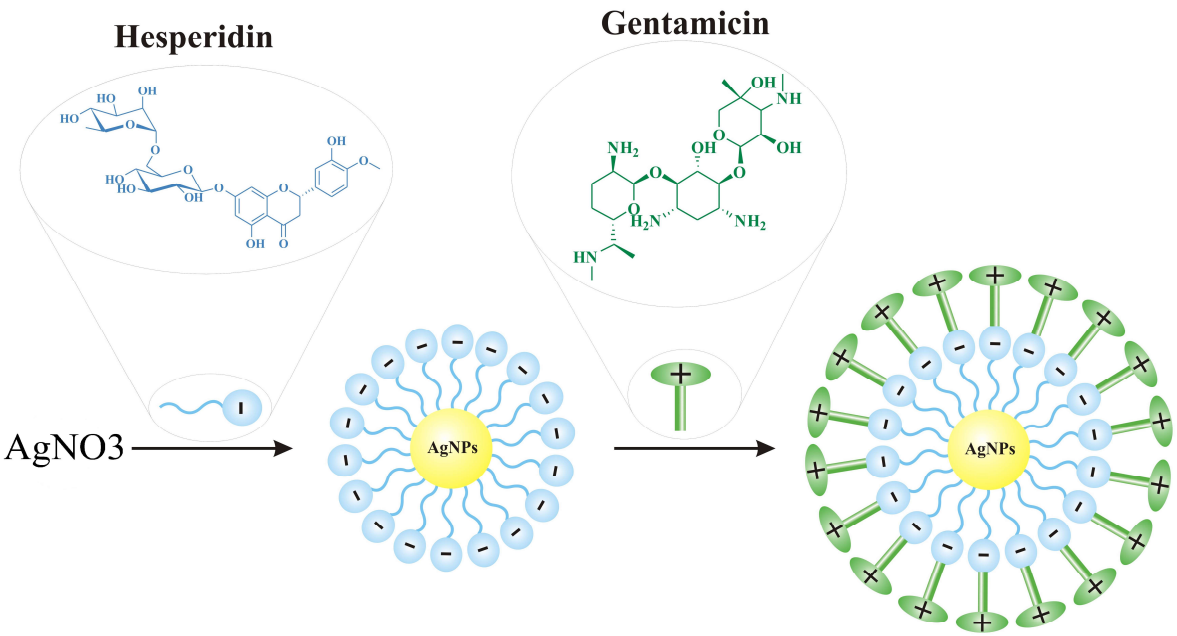

Recognition of GEN by optical nanosensor (HSPAgNPs)

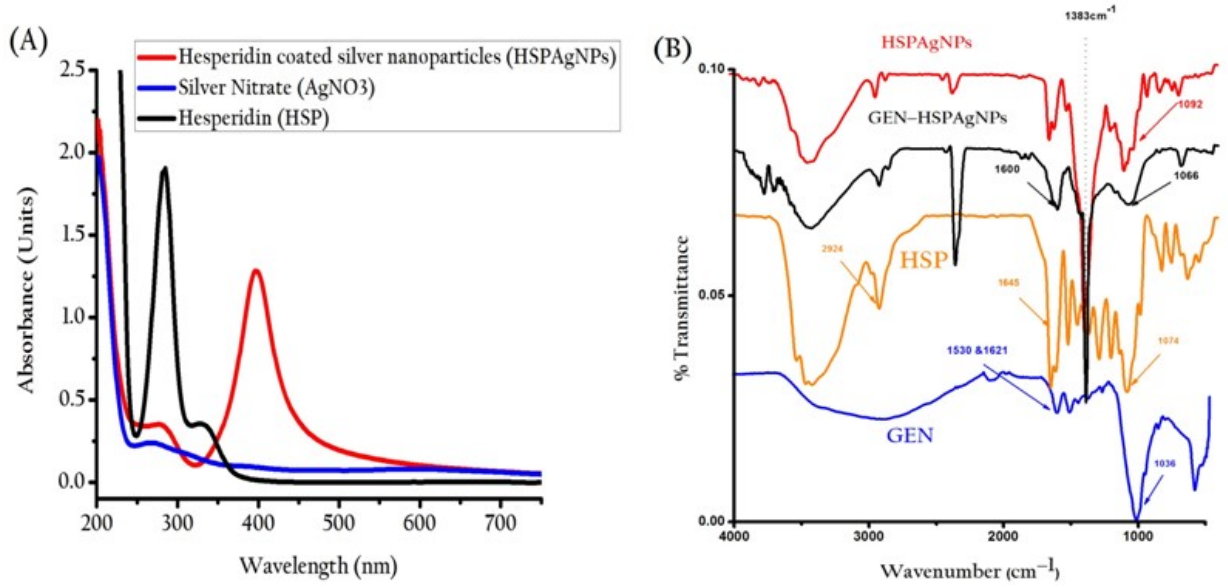

Fig. 1: UV-visible spectra (A) of $AgNO_3$, HSP and HSPAgNPs and (B) FT-IR spectra of HSP, GEN, HSPAgNPs and GEN-HSPAgNPs.

heating (100°C) at hot plate for 15 min and UV-visible spectra was scanned through Shimadzu spectro-photometer (UV-1800) from 190 to 800 nm.

For determination of electrolytic effect of NaCl, five stock solutions of final volume 5.0 ml were prepared in concentration range of 0.1 to 100 mM. An aliquot of 1.0 ml (from each stock solution) was immediately mixed with 1.0 ml of HSPAgNPs (0.1 mM) and behaviour of LSPR band at λ_{max} 398 nm was examined by UV-visible spectroscopy.

A digital pH meter (Eutech, Oakton model-510), comprising a glass indicator and Ag/AgCl reference electrode was used to perform pH study. The original pH of HSPAgNPs was first monitored and then wide range of acidic and alkaline pH (1-13) was maintained by subsequent addition of HCl or NaOH and catastrophic effect on LSPR band of HSPAgNPs was examined by UV-visible spectroscopy.

Determination of HSP content of HSPAgNPs

For UV-visible quantification, about 2 ml solution of HSPAgNPs was centrifugated at 10000 rpm for 30 min. The resultant supernatant was collected and free HSP content was analyzed at λ_{max} 285 nm. A calibration curve was constructed in the concentration range of 0.0625-0.00391 mg/ml and amount of HSP loaded to HSPAgNPs was calculated by formula

% loaded compound = (amount loaded /total amount used) × 100

SEM, FT-IR and DLS analysis

The lyophilized samples of HSPAgNPs and GEN-HSPAgNPs were mounted on metal stubs up to 300 Å with gold sample coater (target of gold model-JFC-1500) and topographical images were recorded by SEM JSM-6380A (JEOL, Japan). FT-IR spectra of HSP, GEN, HSPAgNPs, and GEN-HSPAgNPs were recorded in mid IR-range (400–4000 cm^{-1}) by Bruker Vector 22 spectrometer making potassium bromide (KBr) pellets. The average particle size, PDI and zeta potential of 100 µM solution of HSPAgNPs and GEN-HSPAgNPs was determined using disposable cuvette and dip cell respectively by DLS; Nano-ZSP (Malvern Instruments).

UV-visible screening of pharmaceutical drugs

The recognition behaviour of HSPAgNPs was evaluated for a variety of antimicrobial drugs by mixing equimolar (100 µM) solutions of both (HSPAgNPs & tested drug) in equal proportions. UV-visible spectra of azithromycine, carbamuzeplue, cefixime, ceftriaxone sodium, cefuroxime, cefaclor, cephalexin micronized, clarithromycin, clindamycin phosphate, diclofenac sodium, flurbiprofen, fluconazole, GEN, phenobarbital, prednisolone, and theophylline were recorded instantly, after mixing, followed by vigorous shaking.

Determination of LOD and LOQ for GEN

A univariate concentration study was performed by keeping the concentration of HSPAgNPs constant, meanwhile varying the concentration of GEN gradually in range of 5 to 100 µM. Sequentially, for construction of calibration curve absorbance ratio at 398 nm was plotted as a function of GEN concentration. The approximate limit of detection (LOD) and limit of quantification (LOQ) of GEN was calculated by standard deviation of the ordinate intercept and slop of the regression line by formula: LOD/LOQ = (F x SD) / b where, F = 3.3 and 10 for LOD and LOQ respectively.

SD = standard deviation of the ordinate intercept.

b = slope of the regression line (Shrivastava and Gupta, 2011).

Determination of complexation stoichiometry

Job's method was used to determine the binding stoichiometry of complex between HSPAgNPs and GEN (Shah *et al.*, 2017).

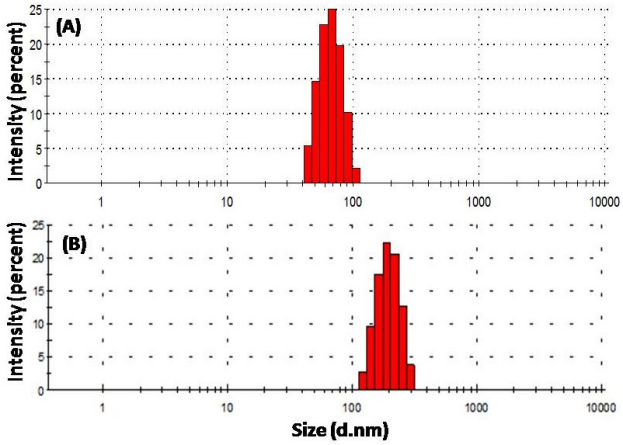

Fig. 2: The relative size distribution (A) of HSPAgNPs and (B) GEN-HSPAgNPs

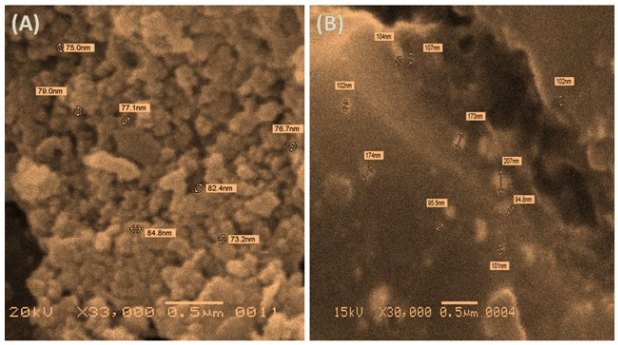

Fig. 3: Scanning electron micrographs (A) of HSPAgNPs and (B) GEN-HSPAgNPs.

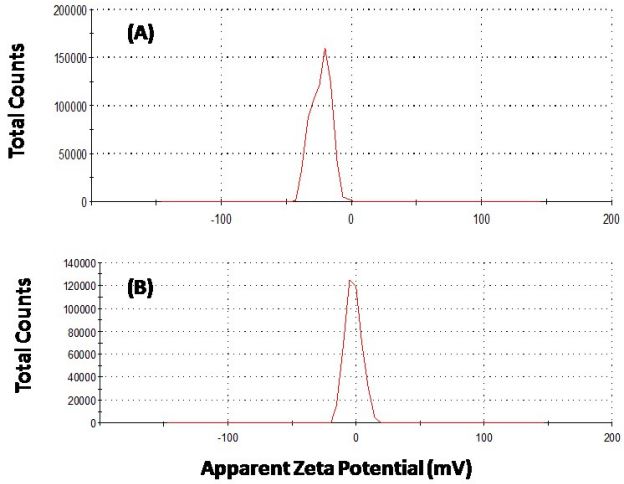

Fig. 4: Zeta potential distribution (A) of HSPAgNPs and (B) GEN-HSPAgNPs**.**

Spiking in tap water, serum, human blood plasma and urine

Blood sampling, preservation, plasma separation via centrifugation (4000 rpm for 5 min at 25°C), serum separation via refrigerated centrifugation (2000 rpm for 10 min) and analysis were carried out (as reported earlier) after taking an approval from ethical committee of the institute (Ateeq *et al.,* 2015; Ikram *et al.,* 2018).

Similarly, for practical applications a sample of human urine (first morning clean middle) was collected and centrifugated (12000 rpm for 10 min at 25°C). 1.0 ml solution of HSPAgNPs and GEN both (100 µM) were added to 1.0 ml of five times diluted resultant supernatant (Ul Ain *et al.,* 2019).

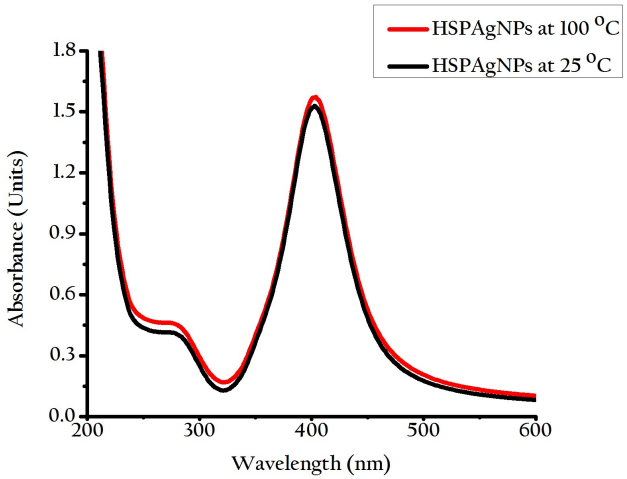

Fig. 5: UV-visible spectra before and after heating of HSPAgNPs.

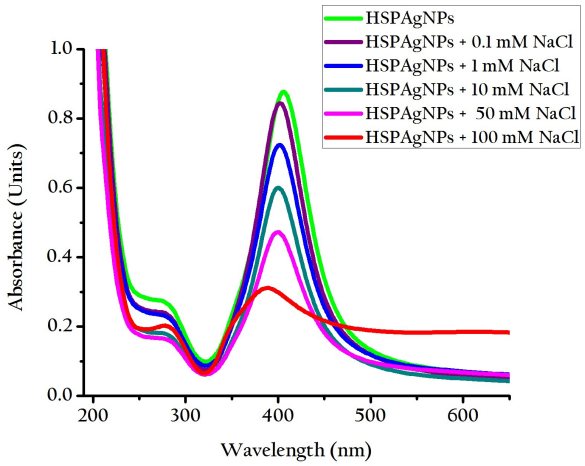

Fig. 6: UV-visible spectra for electrolytic effect of HSPAgNPs

For plasma and serum study two stock solutions (separately for each) of final volume 5.0 ml were prepared in deionized water comprising 1.0 ml of either serum or plasma in 1.0 ml of HSPAgNPs (100 µM), whereas one of the stock solution was without GEN while the second stock solution was prepared by spiking with 1.0 ml aliquot of (100 µM) GEN solution. In order to perform tap water study a solution of GEN (100 µM) was prepared in tap water collected from University of Karachi. Total three stock solutions using tap water were prepared. First two stock solution having final volume 3.0 ml contain 1.0 ml aliquot of HSPAgNPs and GEN both (100 µM) in each respectively, while third stock solution was prepared by mixing 1.0 ml of HSPAgNPs (100 µM), GEN (100 µM) and tap water (Ul Ain *et al.,* 2018).

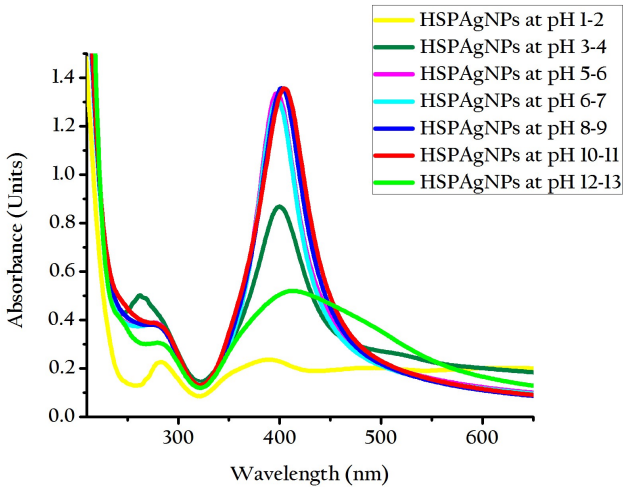

Fig. 7: UV-visible spectra showing effect of varying pH on stability of HSPAgNPs

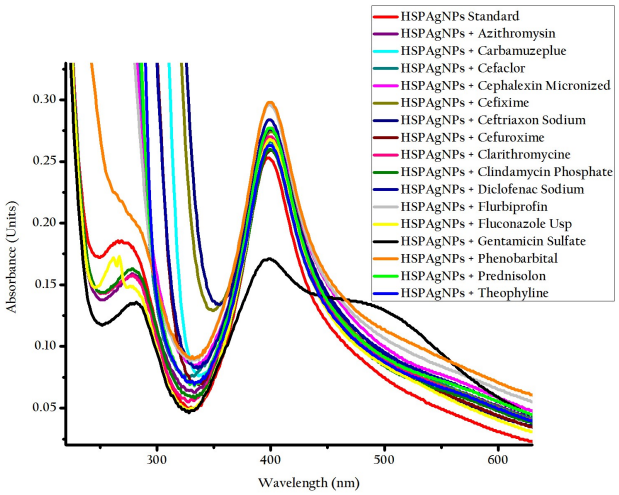

Fig. 8: UV-visible spectroscopic screening of HSPAgNPs with antibiotic drugs.

STATISTICAL ANALYSIS

Instruments e.g., Malvern NanoZSP, the particle size analyzer, etc., used in study are capable of calculating the results along with the statistical treatment. MS Excel® worksheet was used for other Statistical Analyses.

RESULTS

The UV-visible spectra $AgNO_3$, HSP, and HSPAgNPs are shown in fig. 1A. As per UV-visible quantification of HSPAgNPs, about 39% by weight of initial amount of HSP was utilized in the stabilization of AgNPs. Comparative FT-IR spectra of HSP, GEN, HSPAgNPs, and GEN-HSPAgNPs are shown in fig. 1B. The histogram of HSPAgNPs and GEN-HSPAgNPs showed

an average diameter (z-average ± standard deviation) of 77.37±14.24 nm (fig. 2A) and 198.5±16.47 nm (fig. 2B) with PDI of 0.358 and 0.379, respectively. The SEM micrographs revealed that size distribution of HSPAgNPs is ranging from 73.2–84.8 nm (fig. 3A) as compared to GEN-HSPAgNPs having an apparent size of 94.8–207.0 nm (fig. 3B). The surfaces of HSPAgNPs and GEN-HSPAgNPs possessed negative charge (mean value ± standard deviation) i.e., -23.5±7.44 and -2.05±6.29 mV, respectively, as exhibited by zeta potential distribution (fig. 4A and 4B).

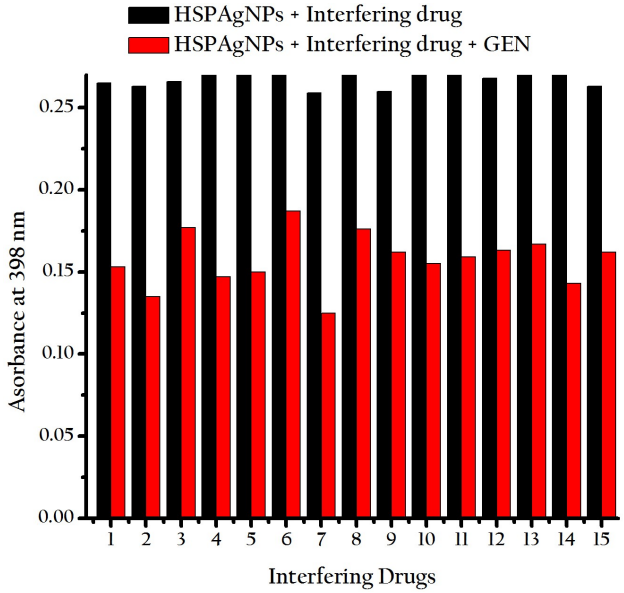

Fig. 9: Selective recognition of GEN by HSPAgNPs in the presence of other common interfering drugs1=azithromycine, 2=carbamuzeplue, 3=cefaclor, 4=cephalexin micronized, 5=cefixime, 6=ceftriaxone sodium, 7=cefuroxime, 8=clarithromycin, 9=clindamycin phosphate, 10=diclofenac sodium, 11=flurbiprofen, 12=fluconazole, 13=phenobarbital, 14=prednisolone, 15=theophylline.

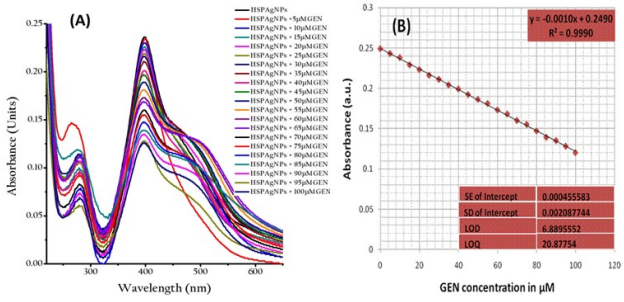

Fig. 10: UV-visible spectra (A) of various concentration of GEN with HSPAgNPs and (B) LOD & LOQ for amount of GEN at 398nm.

The effects of heating, concentration of electrolyte, and pH on HSPAgNPs are shown in fig. 5, 6 and 7, respectively. Profiles of screening of HSPAgNPs with antibiotics and recognition of GEN with HSPAgNPs are given in fig. 8 and 9, respectively. UV-Visible spectra of univariate concentration study are shown in fig. 10A. Consequently, a calibration curve with linear correlation factor R^2 equal to 0.9990 is shown in fig. 10B, which particularize the LOD (6.89 µM) and LOQ (20.88 µM) for HSPAgNPs based on colorimetric detection of GEN. However, the current study is also compared with analytical methods reported in literature as given in table 1. The Job's plot reveals that binding stoichiometry of GEN-HSPAgNPs complexation was 1:2 (fig. 11). The complexation behaviour of HSPAgNPs with GEN over pH range (1–14) is presented in fig.12 showing that original pH of complex GEN-HSPAgNPs is 6.03. UV-Visible spectra of HSPAgNPs and GEN-HSPAgNPs in different real samples, i.e., human blood plasma, urine, serum and tap water are shown in fig. 13.

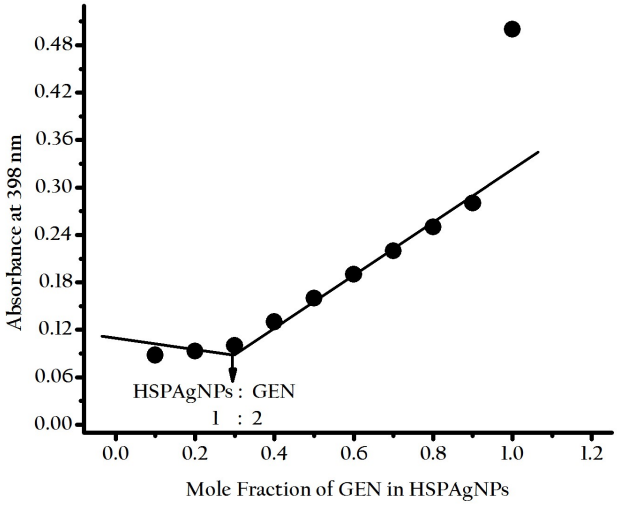

Fig. 11: Job's plot for GEN-HSPAgNPs complexation.

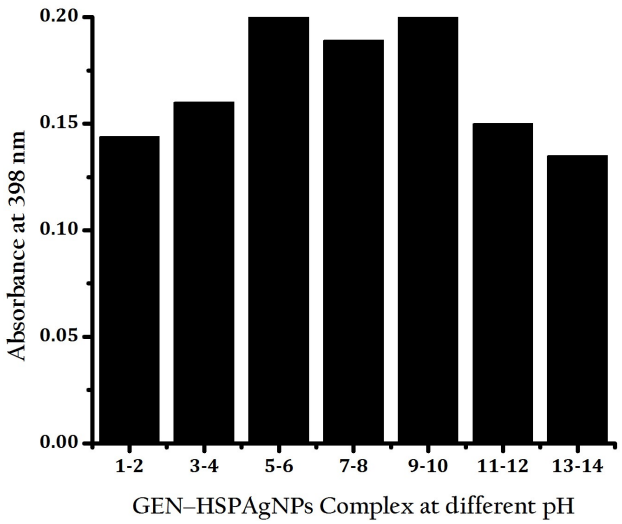

Fig. 12: Optimization of pH for GEN-HSPAgNPs complexation.

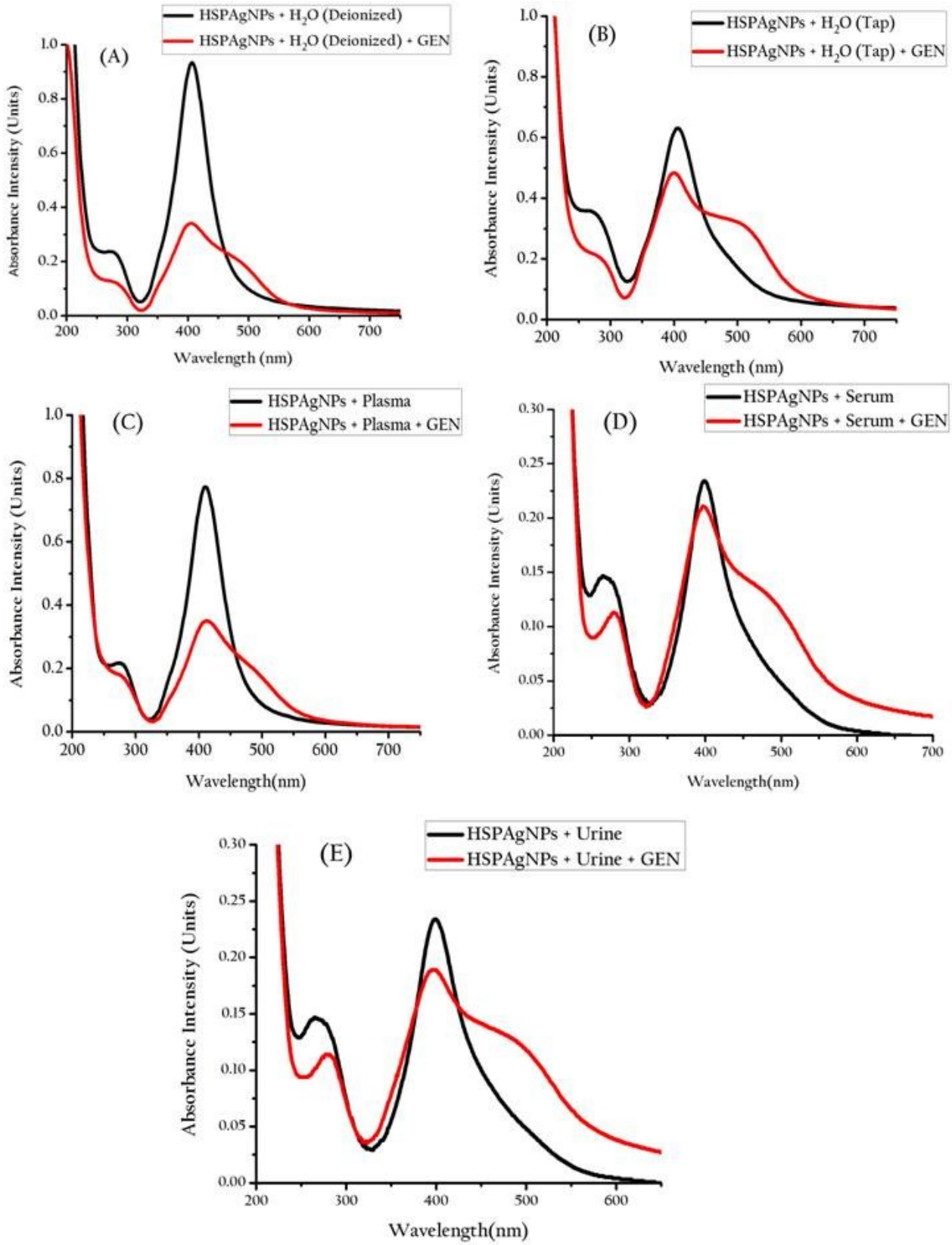

Fig. 13: UV-visible spactra of HSPAgNPs and GEN-HSPAgNPs in (A) deionized water (B) tap water (C) human blood plasma (D) serum and (E) urine.

Table 1: Comparison of reported analytical procedures with the current study for detection of GEN.

Methodology	Analytical ranges	LOD	LOQ	Comments	Reference
Electrochemical method	0.2-50 µg/mL	1.714 µg/mL	6.420 µg/mL	Expensive as well as specific boron-doped diamond electrodes are required	(Abt *et al.,* 2016)
Capillary electrophoresis	2-6 mg/mL	0.67 mg/mL	2.09 mg/mL	Limitation of analytical range Specific background electrolyte is required for baseline correction	(Curiel *et al.,* 2007)
HPLC	4-80 µg/mL	1 µg/mL	8 µg/mL	Fluorimetric detection along with, OPA an off-line derivatizing-agent is required	(Somé *et al.,* 2004)
RP-HPLC	0.001-0.2025 mg/mL	0.37%	0.74%	Expensive instrumentation specific CAD detector is required	(Joseph and Rustum, 2010)
Gentamicin-ninhydrin complexation	2.0-8.0 mg/mL	0.016 mg/mL	0.196 mg/mL	Tedious procedure, pre-complexation is required	(Ismail *et al.,* 2016)
Colorimetry/ HSPAgNPs	5-100 µM	6.89 µM	20.88 µM	Remarkably potent and greener-analytical approach, absolutely devoid of pre-treatment steps required for laboratory/bulk sampling, rapid and short detection time	This study

DISCUSSION

Nutraceutical based nanosensors have been widely explored for colorimetric detection of antibiotic drugs due to their unusual optical properties as well as superiority in exhibiting physical and chemical attributes. In current study, HSP isolated from *C. reticulata* was successfully exploited for robust, environmental friendly, one pot green synthesis of HSPAgNPs. Further, this newly synthesized optical nanosensor eventually served as a colorimetric probe for selective recognition of GEN in presence of various antimicrobial agents.

It has been practically demonstrated that the presence of phenolic groups in the C_6-C_3-C_6 backbone of HSP makes it an ideal candidate for reduction of silver ions and stabilization of AgNPs. Conversion of colourless solution to yellow indicated the formation of HSPAgNPs that gave a characteristic LSPR band at 398 nm, instantly (fig. 1A). It is reported that typically, AgNPs exhibit λ_{max} (absorption maxima) between 350 to 450 nm (Mulfinger *et al.,* 2007).

Interpretation of comparative FT-IR spectra of HSP, GEN, HSPAgNPs and GEN-HSPAgNPs, justified the conjugation of HSP to AgNPs and complexation with GEN. The formation of HSPAgNPs was also identified by the bathochromic shifts indicating the conjugation of HSP (using -OH groups) with Ag^{+1} ions of $AgNO_3$. The FT-IR spectra of HSP (KBr disk) showed characteristics peaks at 3424 cm^{-1} for O-H. Whereas C-H appeared at 2924, C=O at 1645, and C-O at 1074 cm^{-1} (Lahmer *et al.,* 2015). While the FT-IR spectrum of HSPAgNPs, recorded under similar conditions, showed significant hypochromic shifts. Noteworthy, O-H peak shifted from 3424 to 3426 cm^{-1}, indicating involvement of -OH groups of HSP in the stabilization of AgNPs. The characteristic C-O peaks also shifted from 1074 to 1092 cm^{-1}, indicating involvement of Ag^0 in stabilization. Appearance of a new peak at 1383 cm^{-1} corresponding to Ag-O further confirmed the formation of stabilized HSPAgNPs (Rahim *et al.,* 2018). The reference IR spectrum of GEN showed characteristic bands at 1530-1621cm^{-1} corresponding to amide-II and amide-I. A broad diffuse band observed in the range of 2800-3500 cm^{-1} particularly referred to stretching vibrations of alkyl (C-H) and amino (N-H) groups. The absorption peak at 1036 cm^{-1} and 612 cm^{-1} is consonant with HSO_4^{-1} and SO_2 groups of gentamicin sulfate, respectively (Lakdawala *et al.,* 2013; Rapacz-Kmita *et al.,* 2015). FT-IR spectrum of HSPAgNPs loaded with GEN showed a new peak appearing at 1383 cm^{-1}, corresponding to the interaction of GEN with Ag–O bond, confirming formation of GEN-HSPAgNPs complex. Furthermore, a transformation from broad diffuse band (reference spectrum of GEN) to a sharp broad band in the range 2800-3500 cm^{-1} is assignable to chelation of N–H groups of GEN with the free-OH groups of HSP. After complexation the absorption intensity of HSO_4^{-1} group suffers markedly accompanying hypo- as well as bathochromic shifts from 1036 to 1066 cm^{-1} while prominent SO_2 band also shifted and reduced significantly. The characteristic secondary amide-I band

at 1621 cm^{-1} got merged with amide-II bands at 1600cm^{-1}. A comparative FTIR spectrum revealed that complexation (GEN-HSPAgNPs) was achieved by binding of free -OH group of HSP with the -NH_2 groups of GEN, meanwhile the stability of HSPAgNPs gradually suffer due to reduction in number of available -OH groups. Hence, it can be stated that hindrance in the stability of HSPAgNPs ultimately led to enlargement of particle size due to phenomenon of induced-aggregation (fig. 1B).

Findings of DLS indicated that average diameter (z-average ± standard deviation) of HSPAgNPs increased from 77.37±14.24 to 198.5±16.47 nm upon interaction with GEN (fig. 2). The SEM micrographs also validated the consequences of DLS, exhibiting that particle size of HSPAgNPs have increased from 73.2-84.8 to 94.8-207.0 nm after complexation with GEN by virtue of enhanced agglomeration (fig. 3). Surface charges play an important role in term of stability through electrostatic repulsion between particles present in solution phase. Zeta potential values revealed that few negative charges at the surface of HSPAgNPs were neutralized through electrostatic interactions after complexation with GEN, as evident from reduction of net charge (mean value ± standard deviation) from -23.5±7.44 mV to -2.05±6.29 mV (fig. 4).

HSPAgNPs remained stable at room temperature for 30 days without any noticeable shift in LSPR band. HSPAgNPs were found to sustain high temperature up to 100°C for more than 15 min. A negligible reduction in absorbance intensity of HSPAgNPs at 25°C was evident when compared with the UV-visible spectrum at 100°C on exposure of 15 min (fig. 5).

Electrolytic effect of NaCl is one of the important factors involved in the degradation of stability. UV-visible spectra of electrolytic effect exhibited that LSPR band of HSPAgNPs suffers symmetrical hypochromic shift gradually in concentration ranges from 0.1 to 50mM, while the existence of HSPAgNPs demolished at higher concentration of NaCl (100 mM) in response to induced aggregation potential of Cl^{-1} ions (Lakowicz, 1999) (fig. 6).

The Original pH of HSPAgNPs was found to be much closer to neutral pH i.e. 6.52. However, UV-visible spectra of pH study indicated that HSPAgNPs remained stable in pH range of 5-11. The stability of HSPAgNPs significantly effected at highly acidic (1-4) and highly alkaline (12-13) pH (fig. 7).

On the basis of UV-visible screening of pharmaceutical drugs, it was found that none of the drugs (azithromycine, carbamuzeplue, cefixime, ceftriaxone sodium, cefuroxime, cefaclor, cephalexin micronized, clarithromycin, clindamycin phosphate, diclofenac sodium, flurbiprofen, fluconazole, phenobarbital, prednisolon, and theophylline) showed interaction with HSPAgNPs was evident except GEN (as gentamicin sulfate). Noticeable hypochromic shift in LSPR band specifically showed successful interaction between HSPAgNPs and GEN with significantly quenched band at 398 nm. A physical change i.e., transition from characteristic yellow to blackish brown was also observed, when equimolar solutions of both (HSPAgNPs and GEN) were mix together (fig. 8). Moreover, the selective recognition of HSPAgNPs for GEN was also validated in terms of interfering study. Interfering study revealed that in presence of various interfering agents, HSPAgNPs selectively recognized GEN without any significant change in LSPR band (fig. 9).

The elucidation of univariate concentration study displayed a laudable linear relationship (correlation factor R^2, 0.9990) affirming that Beer's law holds good. Furthermore, it also explored the analytical behaviour of HSPAgNPs in terms of LOD and LOQ found to be 6.89 µM and 20.88 µM respectively (fig. 10).

The complexation behaviour of HSPAgNPs with GEN over a wide pH range (1–14) exhibited that HSPAgNPs can act as an excellent nanosensor for GEN in moderately acidic and alkaline environments i.e., in the pH range of 5-10. Hence the comparative trend of pH constraint towards HSPAgNPs and GEN-HSPAgNPs showed that highly acidic and alkaline medium has induced deleterious effects on stability of optical nanosensor by reducing the binding stoichiometry of GEN-HSPAgNPs complex (fig. 11). Therefore, moderately acidic and alkaline conditions are recommended for intended purposes due to sensitivity towards alterations in pH (fig. 12).

Experimental results indicated that the characteristic LSPR band of HSPAgNPs was reproduced in the spiked plasma, serum, urine and tap water. Similarly, after the addition of GEN in HSPAgNPs spiked in plasma, serum, urine and tap water, a distinctive hypochromic shift was observed, showing quenching trend in LSPR band of HSPAgNPs, in analogy to the effect observed in deionized water. Hence, it can be illustrated that the proffered recognition system, HSPAgNPs is potentially effective for selective recognition of GEN in human plasma, serum, urine and tap water (fig. 13).

CONCLUSION

Proposed colorimetric sensor, HSPAgNPs possess remarkable selective recognition potential for GEN in water (laboratory tap and deionized) and biological fluids (plasma, serum and urine), with limit of detection down to 6.89 µM. Moreover, it can be expected that HSPAgNPs based colorimetric detection of GEN in alarming system would be rapid, reliable and potentially conclusive as compared to other methods reported in literature due to short detection time, low detection limit and excellent selectivity.

REFERENCES

Abt B, Hartmann A, Pasquarelli A, Strehle S, Mizaikoff B and Kranz C (2016). Electrochemical determination of sulphur-containing pharmaceuticals using boron-doped diamond electrodes. *Electroanalysis.,* **28**(7): 1641-1646.

Aghel N, Ramezani Z and Beiranvand S(2008). Hesperidin from citrus sinensis cultivated in Dezful, Iran. *Pak. J. Biol. Sci.,* **11**: 2451-2453.

Al-Ahmad A, Daschner F and Kümmerer K (1999). Biodegradability of cefotiam, ciprofloxacin, meropenem, penicillin G, and sulfamethoxazole and inhibition of waste water bacteria. *Arch. Environ. Contam. Toxicol.,* **37**(2): 158-163.

Anastas PT and Warner JC (2000). Green chemistry: Theory and practice.OUP, Oxford, pp.29-75.

Ateeq M, Shah M R, ul Ain N, Ban S, Anis I, Faizi S, Bertino M F and Naz S S(2015). Green synthesis and molecular recognition ability of patuletin coated gold nanoparticles. *Biosens. Bioelectron.,* **63**: 499-505.

Boal AK, Ilhan F, DeRouchey JE, Thurn-Albrecht T, Russell TP and Rotello VM(2000). Self-assembly of nanoparticles into structured spherical and network aggregates. *Nature.,* **404**(6779): 746.

Caruso F, Caruso RA and Möhwald H(1998). Nanoengineering of inorganic and hybrid hollow spheres by colloidal templating. *Science.,* **282**(5391): 1111-1114.

Curiel H, Vanderaerden W, Velez H, Hoogmartens J and Van Schepdael A (2007). Analysis of underivatized gentamicin by capillary electrophoresis with UV detection. *J. Pharm. Biomed. Anal.,* **44**(1): 49-56.

Fang R, Jing H, Chai Z, Zhao G, Stoll S, Ren F, Liu F and Leng X(2011). Study of the physicochemical properties of the BSA: Flavonoid nanoparticle. *Eur. Food Res. Technol.,* **233**(2): 275-283.

Farouk F, Azzazy HM and Niessen WM(2015). Challenges in the determination of aminoglycoside antibiotics, a review. *Anal. Chim. Acta.,* **890**: 21-43.

Greenwood D, Finch R, Davey P and Wilcox M (2007). Antimicrobial chemotherapy. OUP Oxford, pp.98-117.

Hartmann A, Golet E, Gartiser S, Alder A, Koller T and Widmer R (1999). Primary DNA damage but not mutagenicity correlates with ciprofloxacin concentrations in German hospital wastewaters. *Arch. Environ. Contam. Toxicol.,* **36**(2): 115-119.

Heller DN, Clark SB and Righter HF (2000). Confirmation of gentamicin and neomycin in milk by weak cation-exchange extraction and electrospray ionization/ion trap tandem mass spectrometry. *J. Mass Spectrom.,* **35**(1): 39-49.

Ikram F, Qayoom A and Shah MR (2018). Synthesis of epicatechin coated silver nanoparticles for selective recognition of gentamicin. *Sens. Actuators B: Chem.,* **257**: 897-905.

Ingerslev F and Halling-Sørensen B(2000). Biodegradability properties of sulfonamides in activated sludge. *Environ. Toxicol. Chem.,* **19**(10): 2467-2473.

Inoue T, Sugimoto Y, Masuda H and Kamei C (2002). Antiallergic effect of flavonoid glycosides obtained from Mentha piperita L. *Biol. Pharm. Bull.,* **25**(2): 256-259.

Ismail AFH, Mohamed F, Rosli LMM, Shafri MAM, Haris MS and Adina AB(2016). Spectrophotometric determination of gentamicin loaded PLGA microparticles and method validation via ninhydrin-gentamicin complex as a rapid quantification approach. *J. Appl. Pharm. Sci.,* **6**(01): 007-014.

Jin J,Iyoda T, Cao C, Song Y, Jiang L, Li TJ and Zhu DB (2001). Self-Assembly of Uniform Spherical Aggregates of Magnetic Nanoparticles through π–π Interactions. *Angew. Chem.,* **113**(11): 2193-2196.

Joseph A and Rustum A(2010). Development and validation of a RP-HPLC method for the determination of gentamicin sulfate and its related substances in a pharmaceutical cream using a short pentafluorophenyl column and a charged aerosol detector.*J. Pharm. Biomed. Anal.,* **51**(3): 521-531.

Kümmerer K, Al-Ahmad A and Mersch-Sundermann V(2000a). Biodegradability of some antibiotics, elimination of the genotoxicity and affection of wastewater bacteria in a simple test. *Chemosphere*., **40**(7): 701-710.

Kümmerer K, Al-Ahmad A, Wiethan J, Hertle W and Henninger A (2000b). Effects and fate of antibiotics in sewage treatment plants. Proceedings of the Third SETAC World Congress, May, pp.21-25.

Lahmer N, Belboukhari N, Cheriti A and Sekkoum K(2015). Hesperidin and hesperitin preparation and purification from Citrus sinensis peels. *Der. Pharma. Chemica.,* **7**(2): 1-4.

Lakdawala M, Hassan P, Devesh K and Malik G (2013). Poly (D, L-Lactide)-Gentamicin composite coated orthopaedic metallic implant. *Int. J. Sci. Nat.,* **4**(3): 522-529.

Lakowicz JR(1999). Energy transfer. Principles of fluorescence spectroscopy.Springer, pp.367-394.

Liu J, Mendoza S, Román E, Lynn MJ, Xu R and Kaifer AE (1999). Cyclodextrin-modified gold nanospheres. host-guest interactions at work to control colloidal properties. *J. Am. Chem. Soc.,* **121**(17): 4304-4305.

Löffler D and Ternes TA (2003). Analytical method for the determination of the aminoglycoside gentamicin in hospital wastewater via liquid chromatography-electrospray-tandem mass spectrometry. *J. Chromatogr. A.,* **1000**(1-2): 583-588.

McLaughlin LG and Henion JD (1994). Multi-residue confirmation of aminoglycoside antibiotics and bovine kidney by ion spray high-performance liquid chromatography/tandem mass spectrometry. *Biol. Mass Spectrom.,* **23**(7): 417-429.

Mulfinger L, Solomon SD, Bahadory M, Jeyarajasingam AV, Rutkowsky SA and Boritz C (2007). Synthesis and study of silver nanoparticles. *J. Chem. Edu.,* **84**(2): 322.

Naka K, Itoh H and Chujo Y (2003). Temperature-dependent reversible self-assembly of gold nanoparticles into spherical aggregates by molecular recognition between pyrenyl and dinitrophenyl units. *Langmuir.,* **19**(13): 5496-5501.

Patil V, Mayya K, Pradhan S and Sastry M (1997). Evidence for novel interdigitated bilayer formation of fatty acids during three-dimensional self-assembly on silver colloidal particles. *J. Am. Chem. Soc.,* **119**(39): 9281-9282.

Pritchett D and Merchant HE(1946). The purification of hesperidin with formamide. *J. Am. Chem. Soc.,* **68**(10): 2108-2109.

Rahim S, Khalid S, Bhanger MI, Shah MR and Malik MI (2018). Polystyrene-block-poly (2-vinylpyridine)-conjugated silver nanoparticles as colorimetric sensor for quantitative determination of Cartap in aqueous media and blood plasma. *Sens. Actuators B: Chem.,* **259**: 878-887.

Rapacz-Kmita A, Stodolak-Zych E, Ziabka M, Rozycka A and Dudek M (2015). Instrumental characterization of the smectite clay-gentamicin hybrids. *Bull. Mater. Sci.,* **38**(4): 1069-1078.

Saxena A, Tripathi R, Zafar F and Singh P (2012). Green synthesis of silver nanoparticles using aqueous solution of *Ficus benghalensis* leaf extract and characterization of their antibacterial activity. *Mater. Lett.,* **67**(1): 91-94.

Scheurell M, Franke S, Shah R and Huhnerfuss H (2009). Occurrence of diclofenac and its metabolites in surface water and effluent samples from Karachi, Pakistan. *Chemosphere.,* **77**(6): 870-876.

Selimoglu E (2007). Aminoglycoside-induced oto-toxicity. *Curr. Pharm. Des.,* **13**(1): 119-126.

Selke S, Scheurell M, Shah MR and Hühnerfuss H (2010). Identification and enantioselective gas chromatographic mass-spectrometric separation of O-desmethylnaproxen, the main metabolite of the drug naproxen, as a new environmental contaminant. *J. Chromatogr. A.,* **1217**(3): 419-423.

Shah K, ul Ain N, Ahmed F, Anis I and Shah MR (2017). A new highly selective chemosensor for the detection of iron ion in aqueous medium based on click generated triazole. *Sens. Actuators B: Chem.,* **249**: 515-522.

Shenton W, Davis SA and Mann S (1999). Directed self-assembly of nanoparticles into macroscopic materials using antibody-antigen recognition. *Adv. Mater.,* **11**(6): 449-452.

Shrivastava A and Gupta VB (2011). Methods for the determination of limit of detection and limit of quantitation of the analytical methods. *Chronicles Young Sci.,* **2**(1): 21.

Somé IT, Semde R, Moustapha O, Amighi K, Guissou PI, Duez P and Dubois J (2004). Validation of gentamicin congeners using HPLC with electrochemical detection: comparison with fluorimetric detection. *Comptes Rendus Chim.,***7**(10-11): 1087-1093.

Ul Ain N, Anis I, Ahmed F, Shah MR, Parveen S, Faizi S and Ahmed S (2018). Colorimetric detection of amoxicillin based on querecetagetin coated silver nanoparticles. *Sens. Actuators B: Chem.,* **265**: 617-624.

Ul Ain N, Aslam Z, Yousuf M, Waseem WA, Bano S, Anis I, Ahmed F, Faizi S, Malik MI and Shah MR (2019). Green synthesis of methyl gallate conjugated silver nanoparticles: A colorimetric probe for gentamicin. *N. J.C.,* **43**(4): 1972-1979.

Wise R, Hart T, Cars O, Streulens M, Helmuth R, Huovinen P and Sprenger M (1998). Antimicrobial resistance. *BMJ,* **7159**: 317-609.

Zhu YG, Johnson TA, Su JQ, Qiao M, Guo GX, Stedtfeld RD, Hashsham SA and Tiedje JM (2013). Diverse and abundant antibiotic resistance genes in Chinese swine farms. Proceedings of the National Academy of Sciences, pp.3435-3440.